

Numerical Computation and Experimental Measurement of Aerodynamic Noise

Present and Future



Chisachi Kato,
University of
Tokyo

Outline



- Background
- Numerical Prediction of Aerodynamic Noise
- Applications at Present
- Perspectives and Future Roles of Measurements



Background

平成21年9月3日

Prediction and Reduction of Aerodynamic Noise

3



■ Aerodynamic Noise

- Generated from deformation of vortices
- Drastically increase with increasing flow speed

■ Reduction of Aerodynamic Noise

- Crucial in development of various fans, airplane, automobiles, etc.

■ Expectations for Numerical Predictions

- Cost and/or time reduction for prototyping
- Reduction of noise by identifying essential mechanism for noise generation
- Prediction of noise under installation conditions

平成21年9月3日

4



Numerical Prediction of Aerodynamic Noise

平成21年9月3日

5

Direct vs. Decoupled Methods



■ Direct Computation of Aerodynamic Noise

- Provide information regarding detailed mechanism of noise generation
- Applicable to feedback noise
- Limited to simple geometries, particularly for noise from low speed flows

■ Decoupled Methods

- Based on acoustic analogy
- No feedback assumed
- Applicable to relatively complex geometries
- Various methods have been proposed

平成21年9月3日

6



Applications at Present

平成21年9月3日



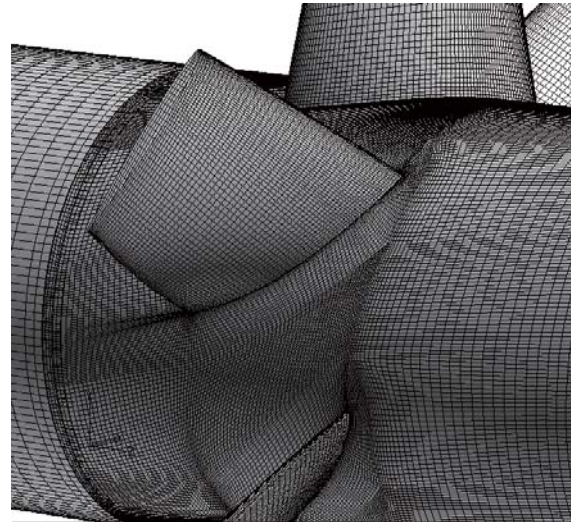
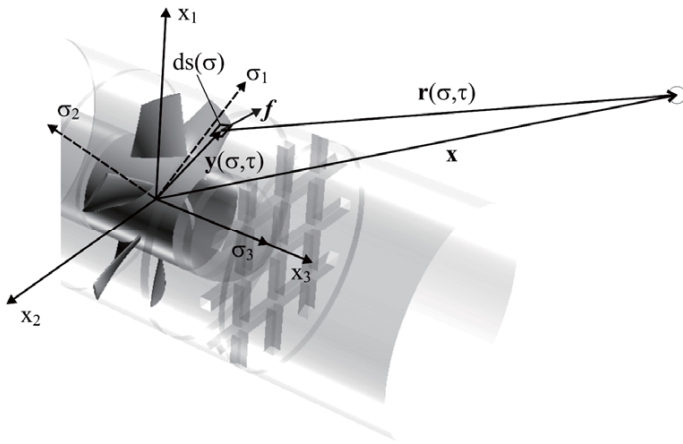
Noise Generated from an Axial-flow Fan Subjected to Inflow Turbulence

Collaborator: Siegen University in Germany

平成21年9月3日



Computational Model



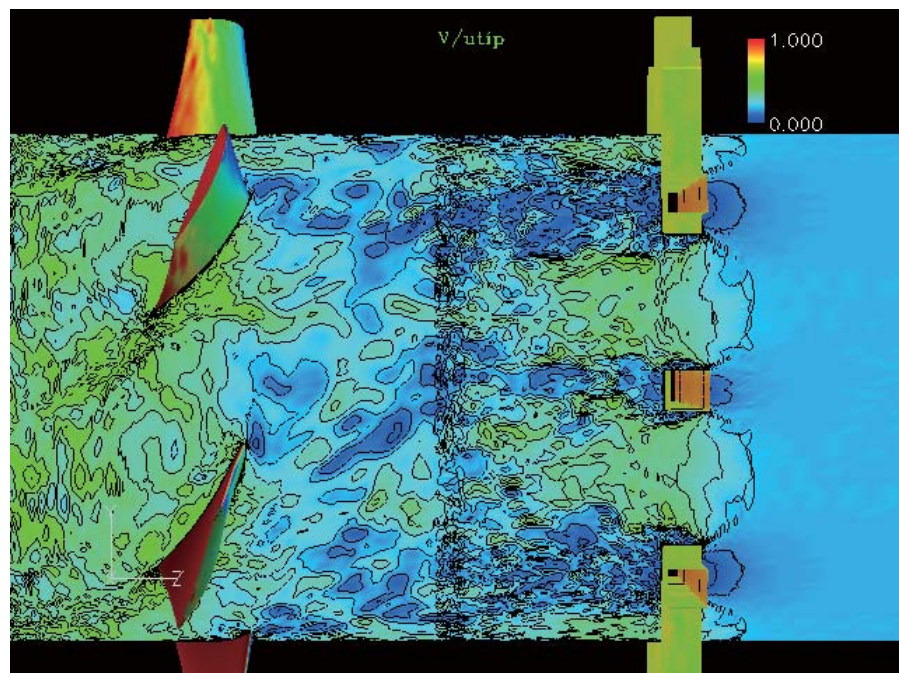
Ducted Fan Subjected to Turbulence Ingestion

Computational Grids on Blade Surface

平成21年9月3日

9

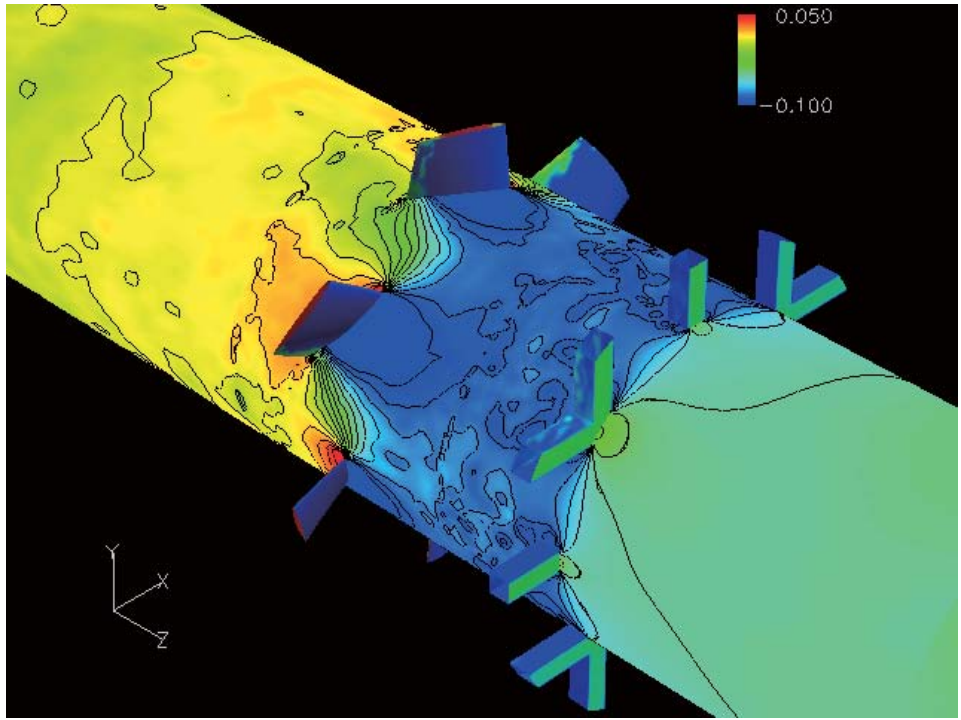
Fluctuations of Instantaneous Streamwise Velocity



平成21年9月3日

10

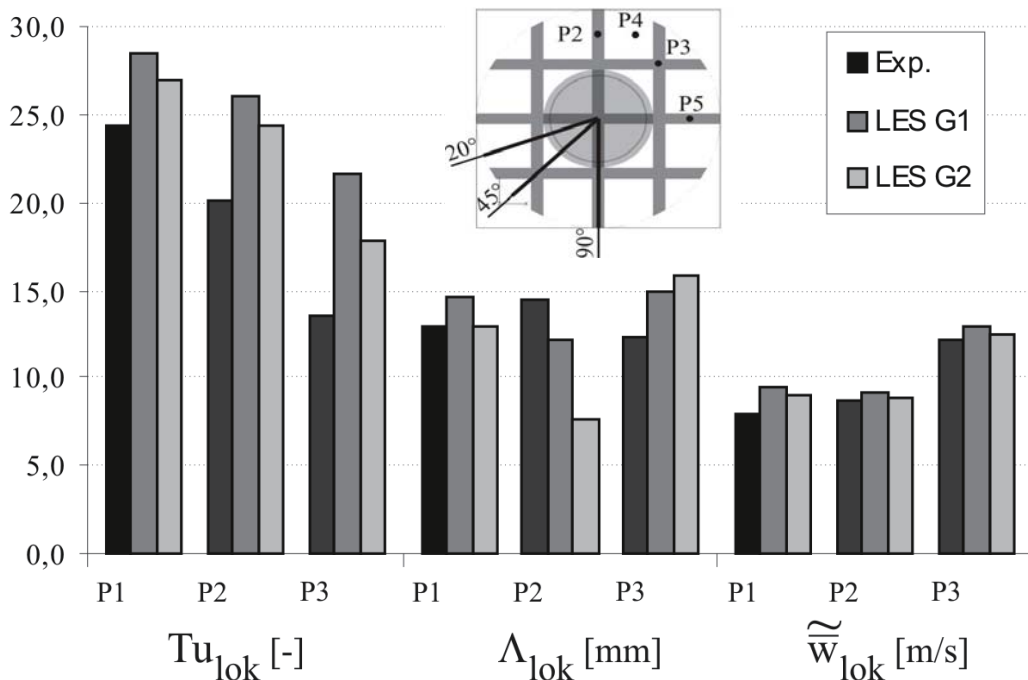
Fluctuations of Instantaneous Static Pressure



平成21年9月3日

11

Comparisons of Turbulence Statistics behind Grid



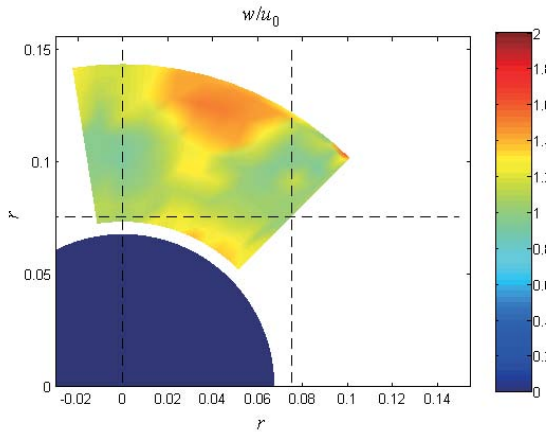
平成21年9月3日

12

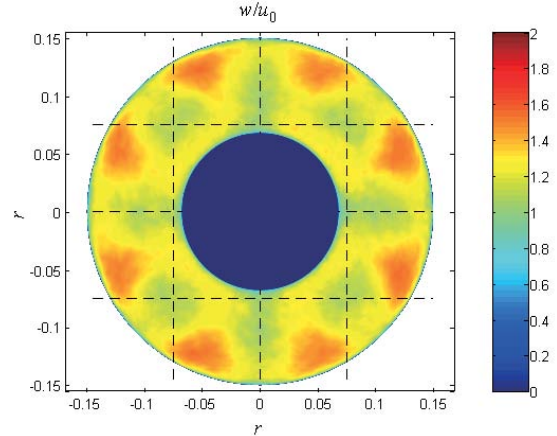
Comparison of Turbulence Intensity behind Grid



■ Incoming Turbulence Intensity



Measured by Hot Wire



Computed by LES

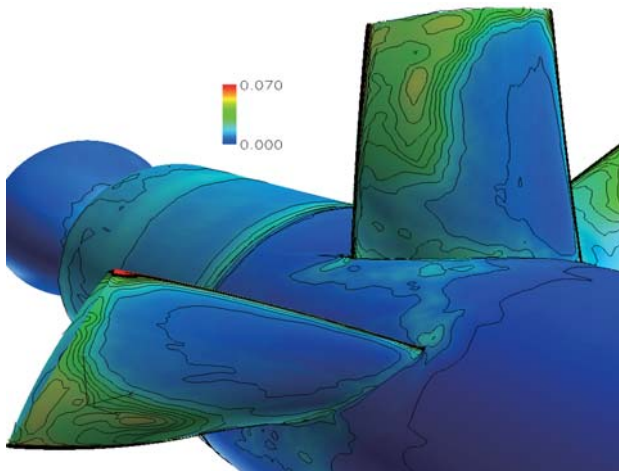
平成21年9月3日

13

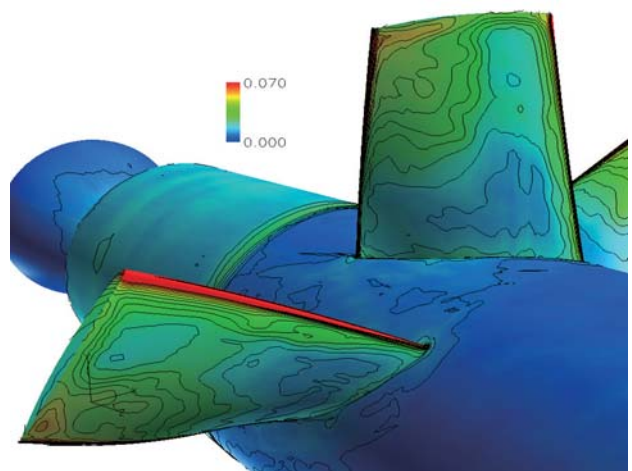
Comparison of Surface Pressure Fluctuations



Root-mean-square Value of C_p



Clean Inflow Case



Turbulent Inflow Case

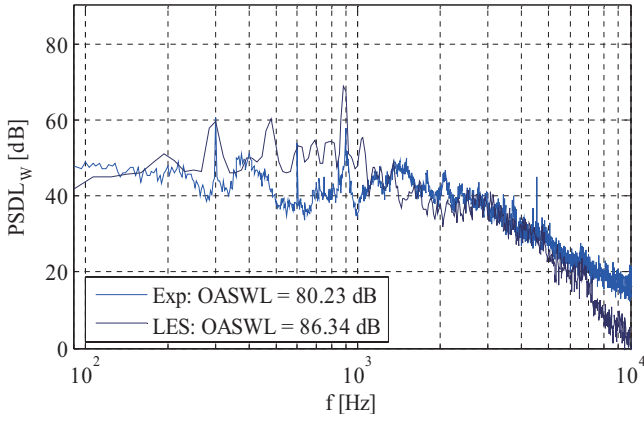
平成21年9月3日

14

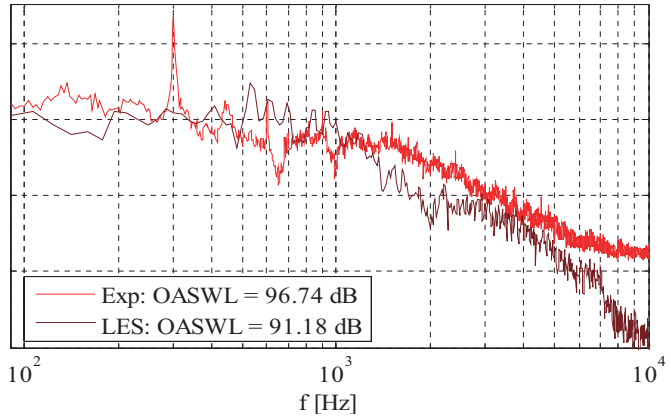
Comparison of Radiated Sound Pressure Levels



Far-field Sound Pressure Level



Clean Inflow



Turbulent Inflow

平成21年9月3日

15

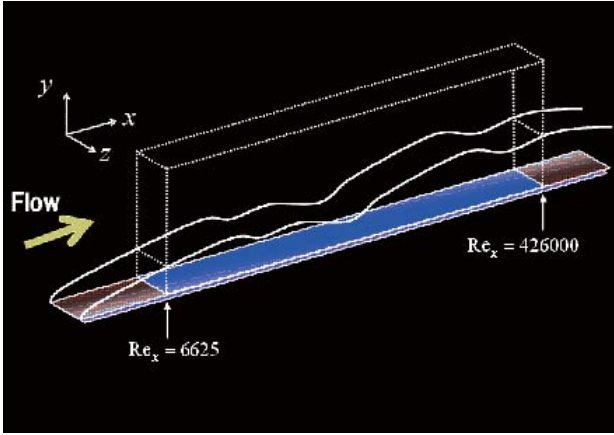


Bypass Transition of Flat Boundary Layer and Resulting Sound

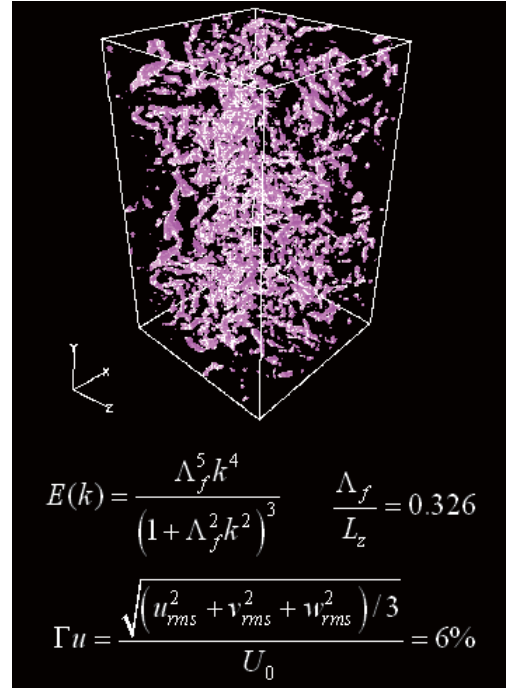
平成21年9月3日

16

Computational Model



	# of nodes	Grid size
x	1134	$\Delta^+ = 14-38$
y	70	$\Delta^+ = 1-76$
z	76	$\Delta^+ = 15$



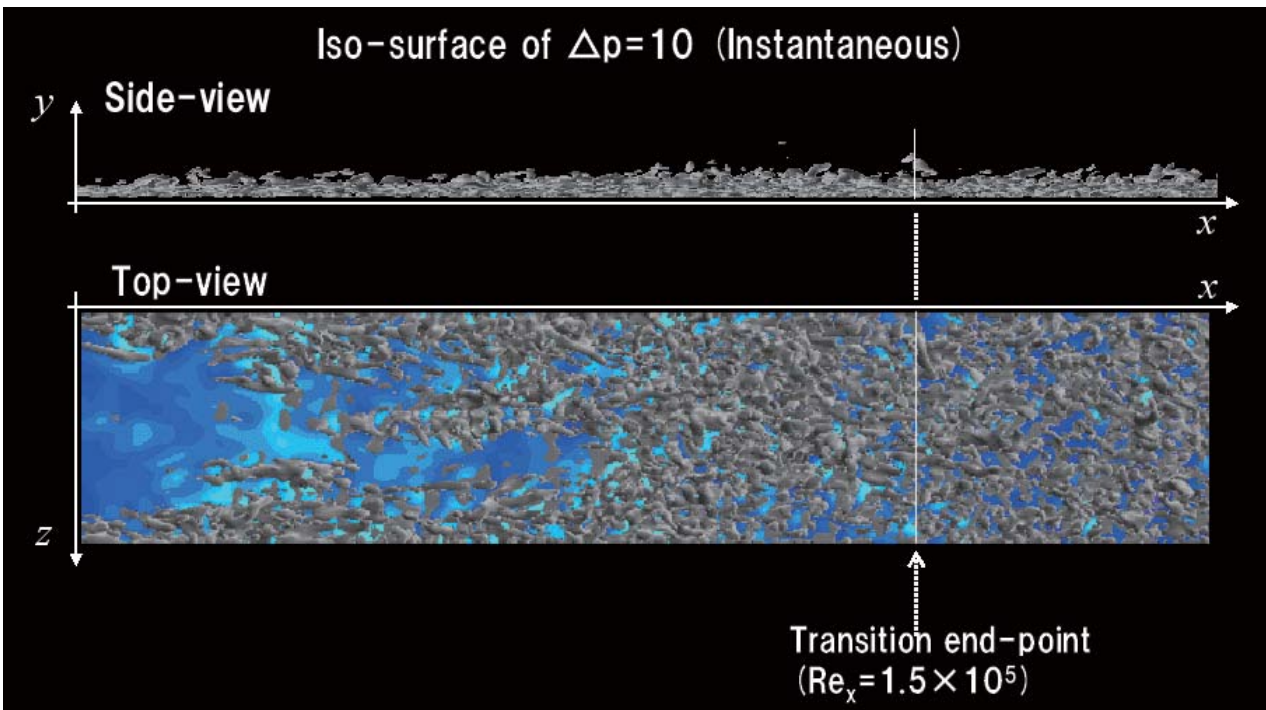
Inflow Turbulence

平成21年9月3日

Grid Resolution

17

Instantaneous Vortical structure

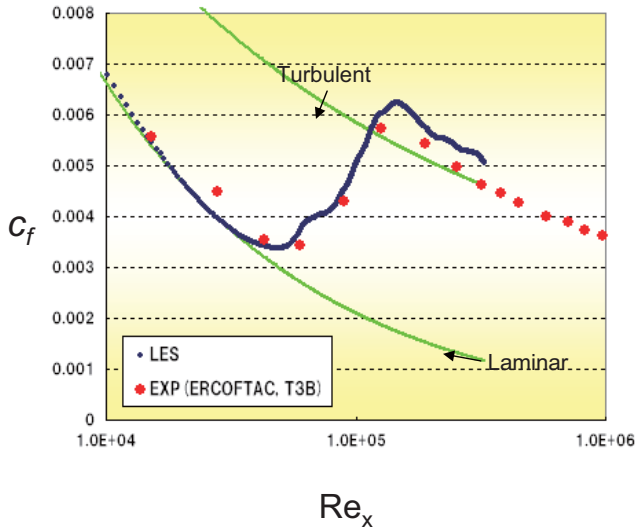


平成21年9月3日

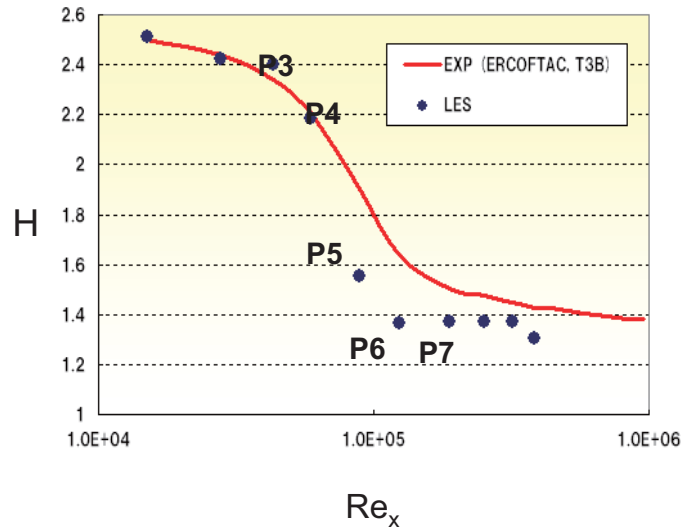
18



Comparison of Skin Friction and Shape Factor



Skin Friction Coefficient



Shape factor

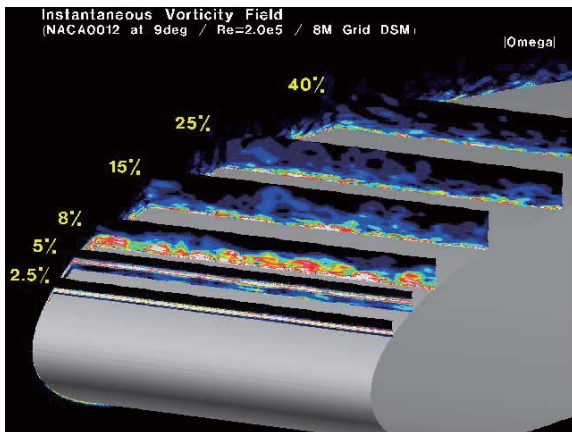
平成21年9月3日

19

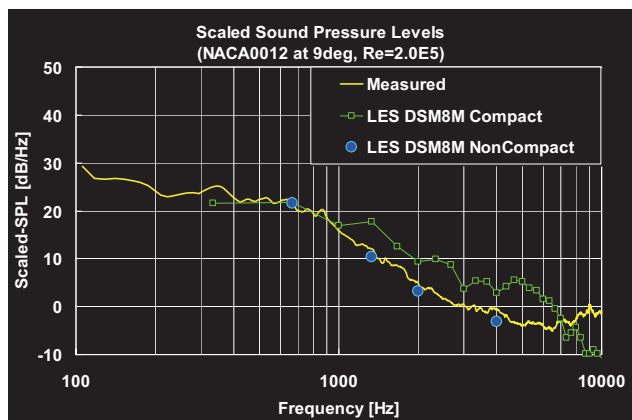
Prediction of Transitional Boundary Layer and Resulting Sound



NACA0012: Angle of attack=9 deg, $Re=2.0 \times 10^5$



Vortical Structure near L. E.

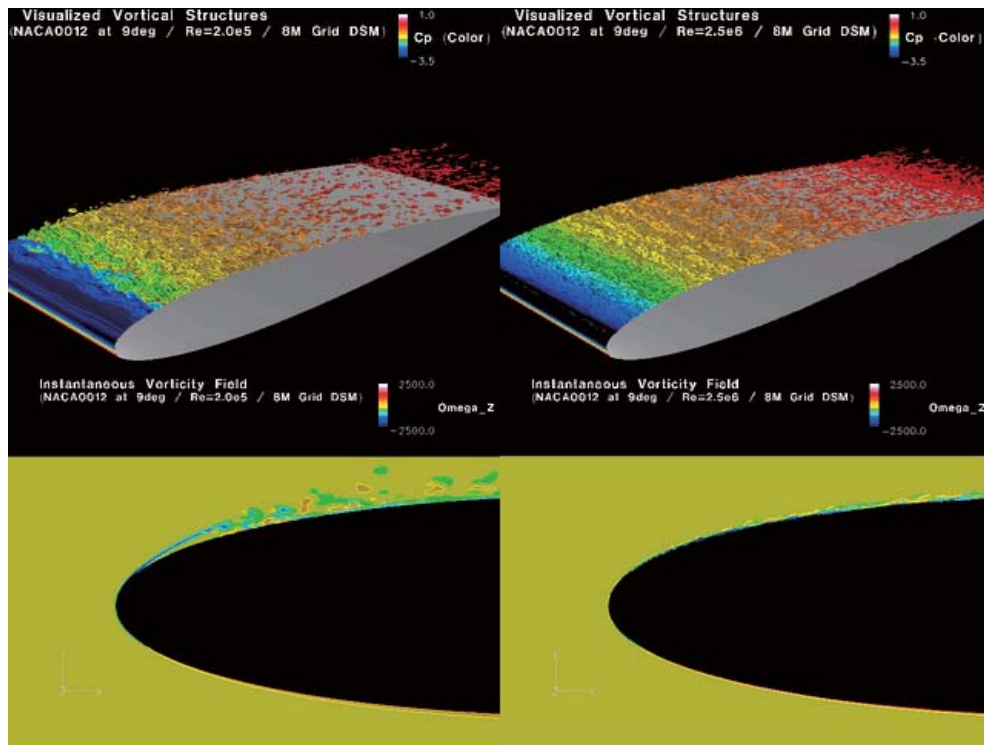


Comparison of Far-field Sound Pressure Level

平成21年9月3日

20

Effects of Reynolds Number on Transition Process (left: 2.0×10^5 , right: 2.0×10^6)



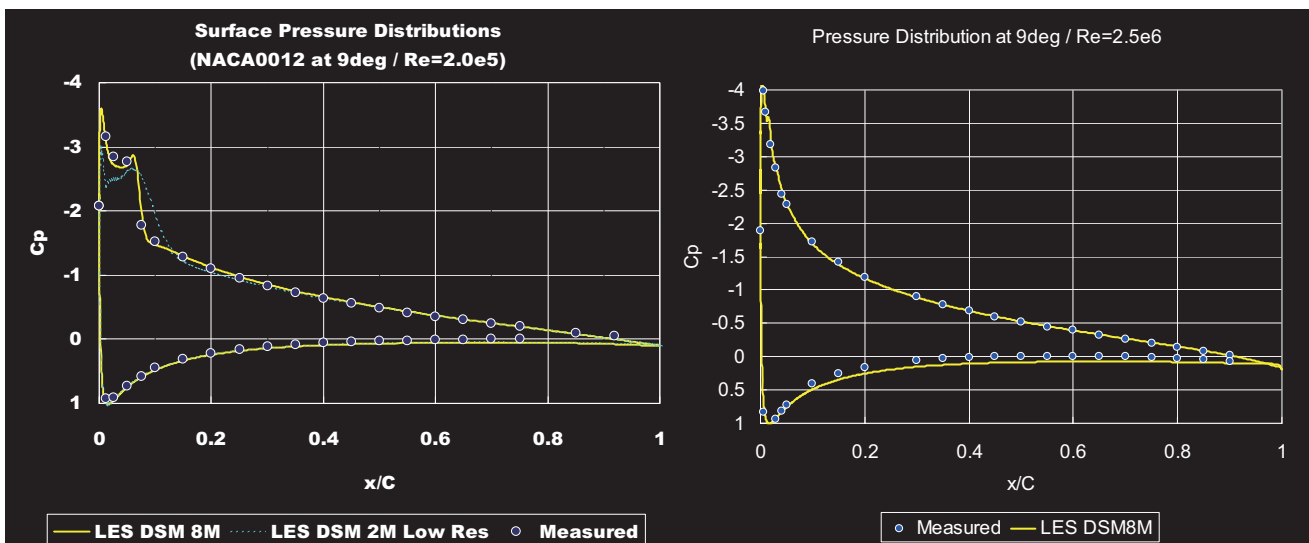
平成21年9月3日

21

Effects of Reynolds Number on Surface Pressure Distributions



NACA0012: Angle of Attack = 9 deg.



■ $Re = 2.0 \times 10^5$
($U_0=20\text{m/s}$, $C=0.15\text{m}$)

■ $Re = 2.5 \times 10^6$
($U_0=50\text{m/s}$, $C=0.75\text{m}$)

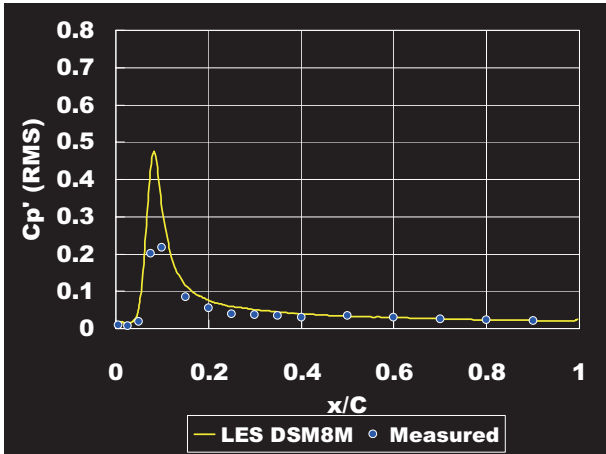
平成21年9月3日

22

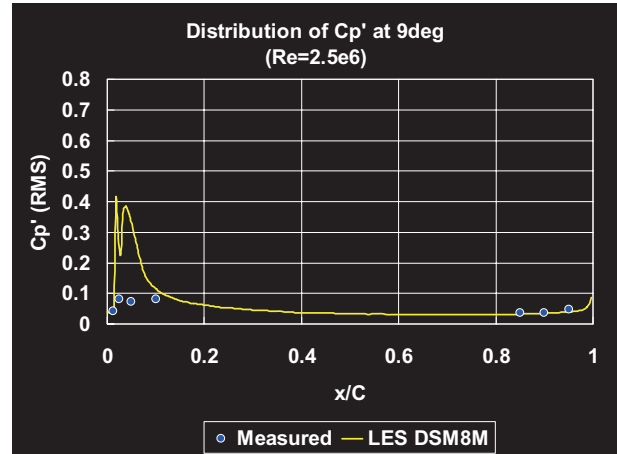
Comparison of Surface Pressure Fluctuations



Angle of Attack: 9 degrees



■ $Re = 2.0 \times 10^5$
($U_0=20\text{m/s}$, $C=0.15\text{m}$)



■ $Re = 2.5 \times 10^6$
($U_0=50\text{m/s}$, $C=0.75\text{m}$)

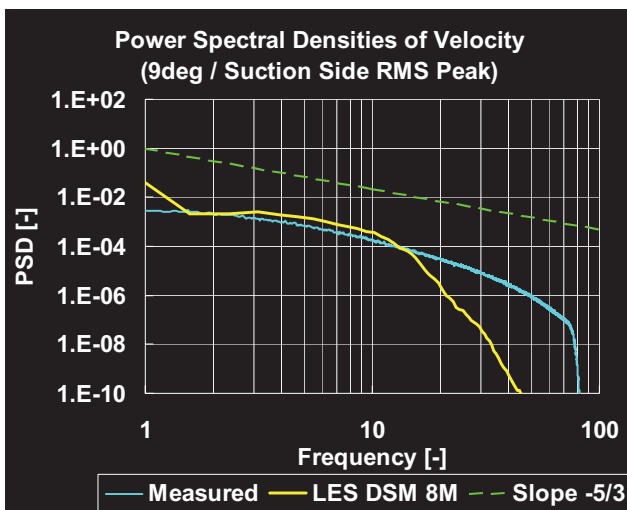
平成21年9月3日

23

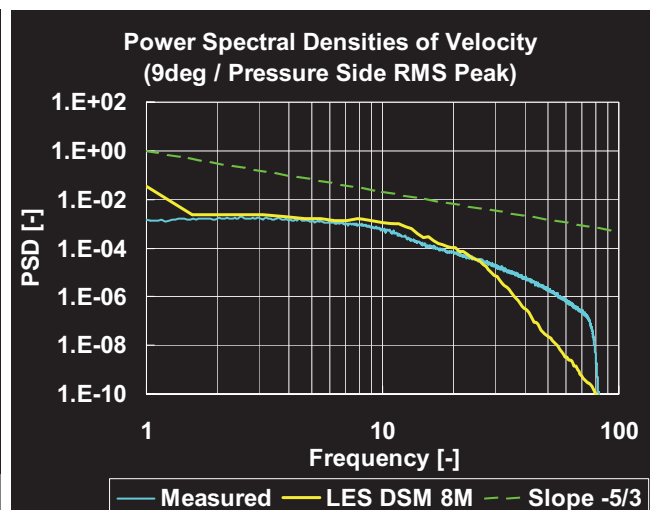
Comparisons of Frequency Spectra of Velocity Fluctuations in Near Wake



Angle of Attack: 9 degrees, $Re = 2.0 \times 10^5$



■ $x/C=1.1$
(suction side)

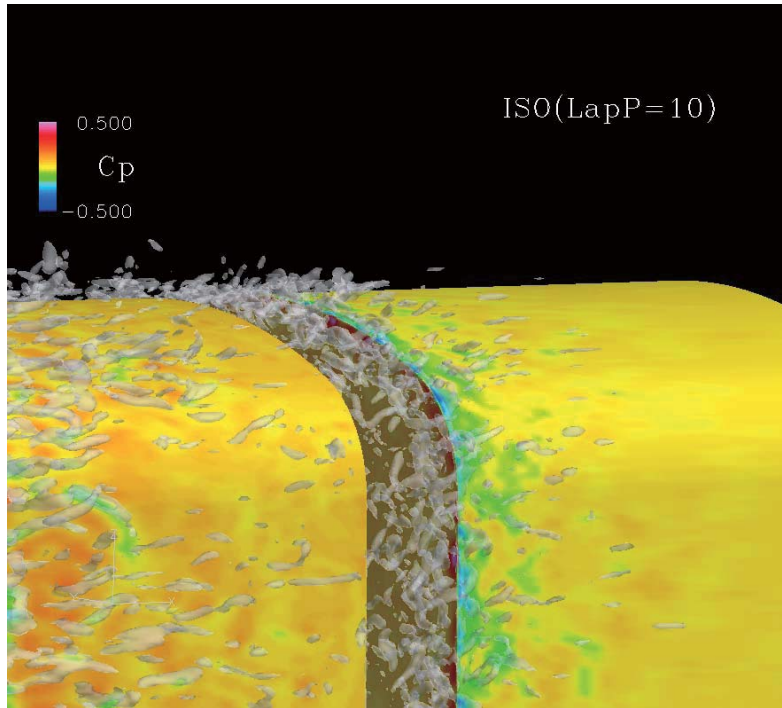


■ $x/C=1.1$
(pressure side)

平成21年9月3日

24

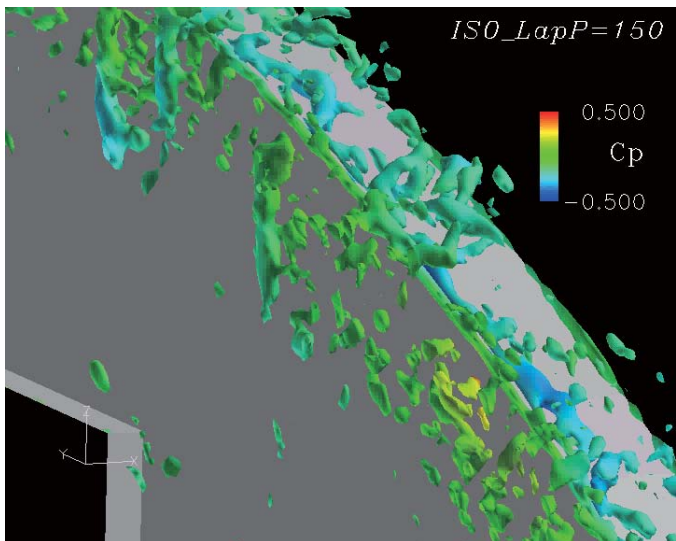
Approaching TBL and Flow in Actual Car Gap



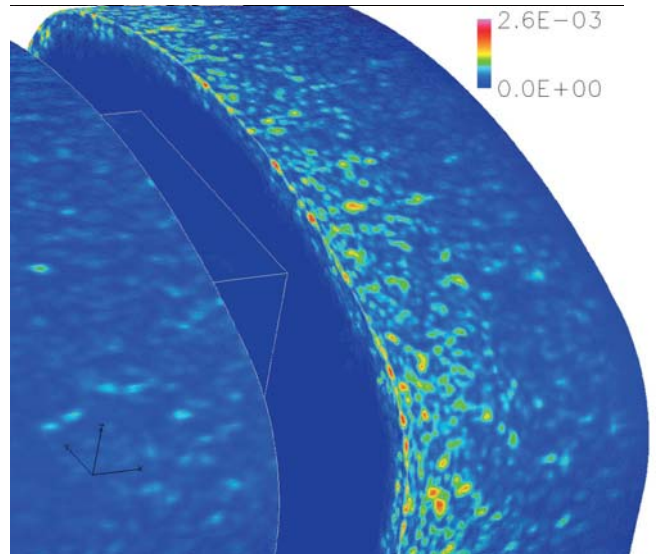
平成21年9月3日

25

Stretching of Vortices and Acoustical Source on Surface



Stretching of Vortices at the Edge



Aeroacoustical Sources at 4.8 Hz

平成21年9月3日

26

26

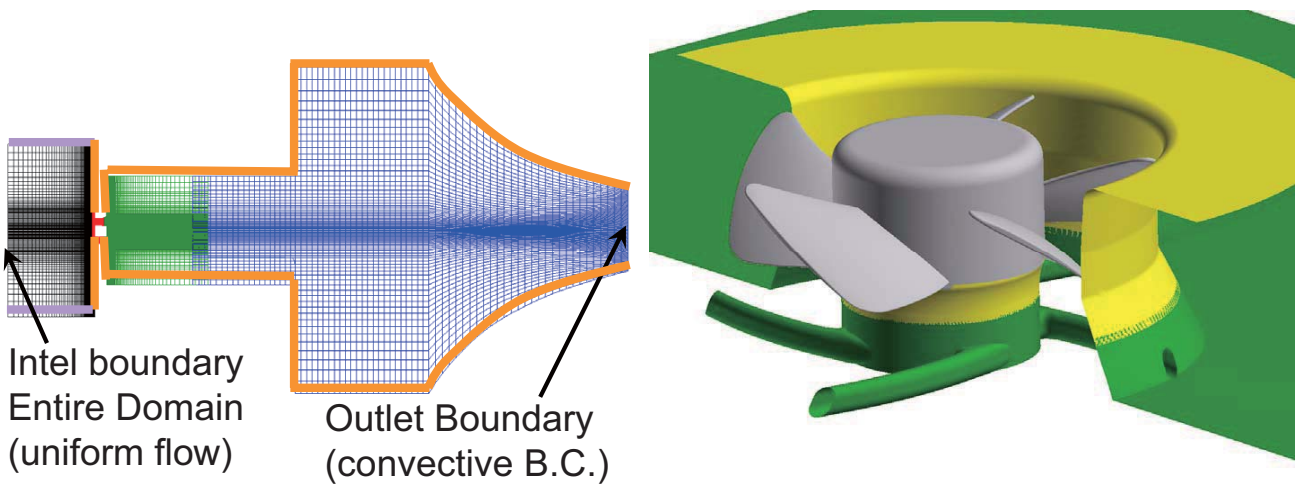


Sound Radiated from a Small Propeller Fan

平成21年9月3日

27

Computational Model and Boundary Conditions



Inlet boundary
Entire Domain
(uniform flow)

Outlet Boundary
(convective B.C.)

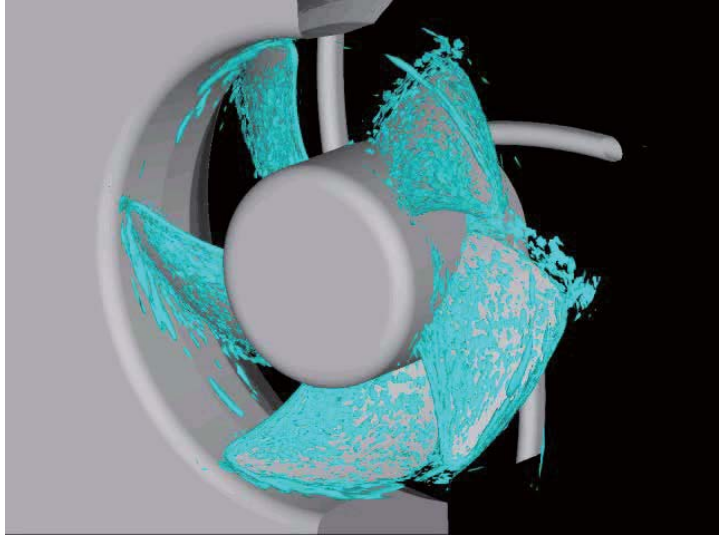
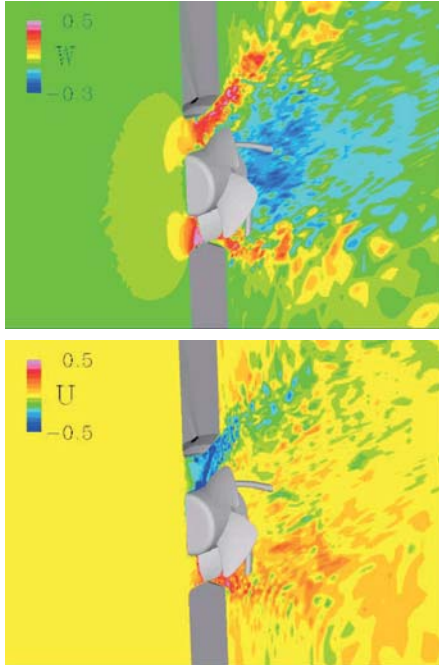
Entire Domain

Near Fan Blades

平成21年9月3日

28

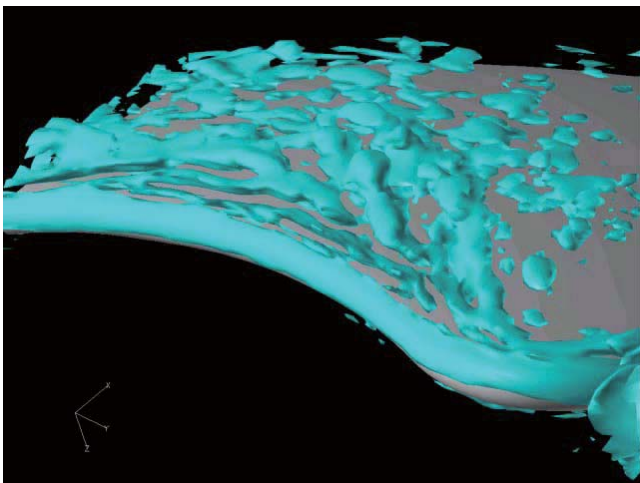
Instantaneous Flow Fields

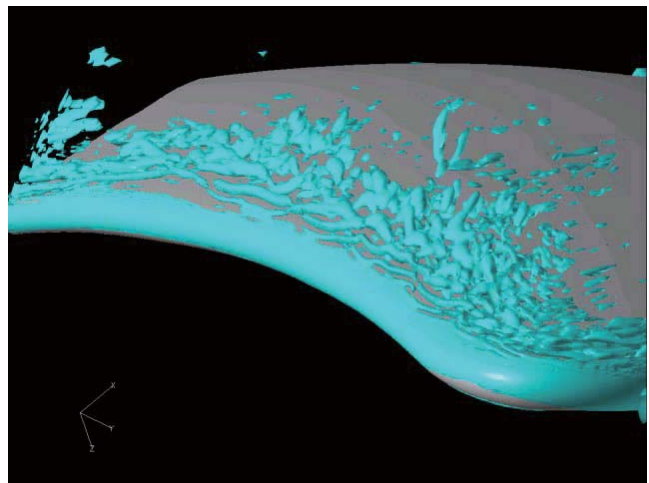
平成21年9月3日

29

Effects of Grid Resolutions

Coarse Mesh



Fine Mesh

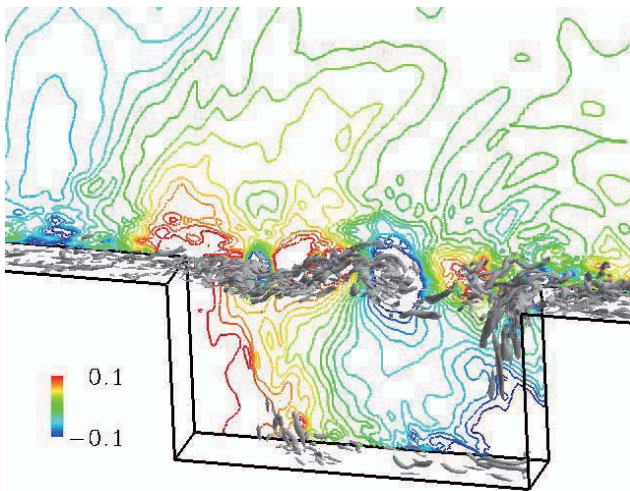
平成21年9月3日

30

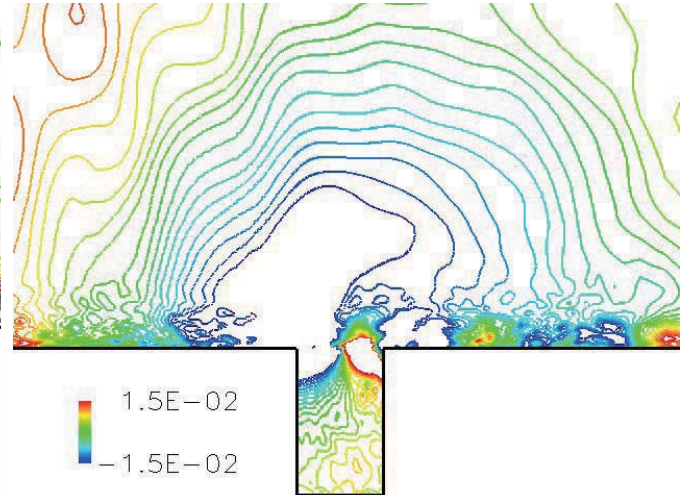
キャビティ音の直接数値解析



■ フィードバック機構の詳細説明



$D/L = 0.5$ ($St = 0.8$)



$D/L = 1.7$ ($St = 0.4$)

平成21年9月3日

31



Perspectives and Future Roles of Measurements

平成21年9月3日

32

Summary



■ Numerical Predictions of Aerodynamic Noise

- will partially replace prototyping and/or model tests up to Reynolds number $O(10^6)$

■ Future Role of Measurements

- Provide accurate and detailed data for validating numerical methods
- Extract Essential Physical Phenomena